Deliverable 3.3

Aqueous-phase reformer – catalyst selection, adaption, and characterization

Author: Paulo Ribeirinha, Paranjeet Lakhtaria, Adélio Mendes (UPorto)

Deliverable due date: 31-03-2023

Deliverable submission date: 31-03-2023

Dissemination Level		
PU	Public	**x**
PP	Restricted to other programme participants (including the Commission Services)	
RE	Restricted to a group specified by the consortium (including the Commission Services)	
CO	Confidential, only for members of the consortium (including the Commission Services)	
CON	Confidential, only for members of the Consortium	

This project has received funding from the Fuel Cells and Hydrogen 2 Joint Undertaking under grant agreement No 871967. This Joint Undertaking receives support from the European Union's Horizon 2020 research and innovation programme, Hydrogen Europe and Hydrogen Europe research.

Table of Contents

1. Summary of scope of report

The methanol APR research has been focused mostly on finding suitable catalysts that promote the reforming reactions at lower temperatures and inhibit undesired reactions. Amongst noble (Pt, Ru) and non-noble (Ni, Cu) metals, Pt and Ni-based catalysts are the most widely used catalysts for methanol APR. University or Porto has previously performed extensive literature review on methanol APR for the selection, characterization, and optimization of the catalysts. As stated previously on the deliverable 3.2, Pt and Ni-based catalysts were selected and optimized to be tested for the EMPOWER CHP system. These catalysts were then tested on a lab-scale methanol APR set-up designed and developed at University of Porto.

2. Experimental procedure

The catalyst performance in methanol APR was measured using a fixed-bed reactor (FBR) (70 mm x 7 mm). A 700 mg of catalyst and an equal amount of glass beads were mixed and loaded into the midsection of a FBR. Glass wool and steel mesh were inserted at both ends of the reactor to avoid dragging catalyst out of the reactor. The reactor was placed vertically inside a temperature-controlled oven and reactants were continuously fed in an upwards direction during APR tests. Before APR tests, catalysts were reduced in-situ under H_2/N_2 (1:1) atmosphere for 2 h at 300 °C. The reactor was then purged with N_2 gas for 30 min (50 mL·min^{-1}) to remove adsorbed H_2 from the catalyst. Methanol APR experiments were conducted at the temperature of 230 °C with N_2 co-feeding (30 mL·min-1) using 5wt. % & 55 wt. % methanol aqueous solution at 3.3 MPa and 6.0 MPa respectively. Aqueous methanol solution was fed to the reactor in an upwards direction by an HPLC pump (KNAUER Smartline Manager 5050) with weight hourly space velocity (WHSV) between 0.1 h^{-1} and 21.2 h^{-1}. The outlet stream from the reactor was cooled down in a condenser at *ca*. 0 °C to separate liquid-phase effluents and gaseous products. The formed gaseous products were measured with online gas chromatography (GC) (Shimadzu GC 2010 Plus) equipped with two columns, Pora-Plot Q (Agilent) and HP-Molesieve (Agilent), and a barrier ionization discharge detector (BID). Catalytic activity in methanol APR was measured in terms of methanol conversion (equation 1) and H_2 production rate (equation 2) and selectivity (equation 3). Herein, *n* denotes the number of moles, $MeOH_{in}$ is inlet methanol steam, $MeOH_{out}$ is outlet methanol steam and $m_{catalyst}$ is the mass of catalyst in grams. All the results presented in this study were measured after achieving steady-state reaction conditions.

$$\text{Methanol conversion (\%)} = 100 \times \left(\frac{n\text{MeOH}_{\text{in}} - n\text{MeOH}_{\text{out}}}{n\text{MeOH}_{\text{in}}}\right) \quad (1)$$

$$\text{H2 production rate (µmol·min-1·gcatalyst-1)} = \frac{n(H_2)}{60 \times m_{catalyst}} \quad (2)$$

$$\text{Selectivity Hydrogen (\%)} = \frac{n(H_2)}{\sum GasProducts_{out}} X\ 100 \quad (3)$$

The methanol-water vapor pressure was obtained for temperatures of 190 °C, 210 °C, and 230 °C, using Aspen Technology. The plot of the bubble pressure versus methanol mole fraction at the three different temperatures is shown in Figure 1. This plot is fundamental to assure that the kinetic characterization of methanol APR using Pt/Al_2O_3 catalyst is properly carried out at all experimental conditions, *i.e.,* with methanol in the liquid phase. As the methanol concentration increases, the required pressure to keep the mixture in a liquid state increase as well. In literature, most experiments were performed using a 5 wt. % methanol aqueous solution, yet commercial HT-PEMFC systems (EMPOWER CHP) that use methanol reformers for in-situ hydrogen production typically run using 55 wt. % methanol aqueous solutions.

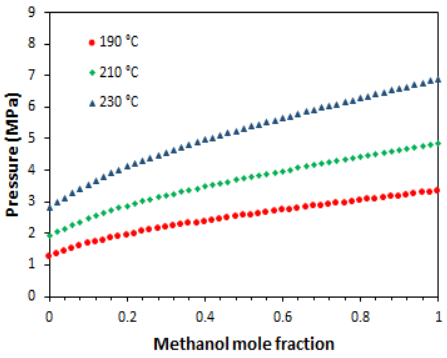

Figure 1. The bubble point pressures of binary methanol-water mixture for the different mole fractions of methanol for temperatures of 190 °C, 210 °C, and 230 °C were predicted using Aspen Technology.

3. Pt/Al_2O_3 catalyst – catalytic activity and stability performance

The performance of Pt/Al_2O_3 was investigated in a temperature range of 190-230 °C with an identical set of feed flow rates. The effect of methanol concentration in feed aqueous solution on the catalyst performance was studied as well. The performance of Pt/Al_2O_3 was characterized in terms of methanol conversion, hydrogen production rate, and hydrogen selectivity. The catalyst (5 wt. % Pt loading) supplied by Sigma-Aldrich in powder form was used without further modification.

3.1. Physicochemical characterization of Pt/Al_2O_3

Hydrogen – temperature-programmed reduction (H2-TPR) and X-ray diffraction (XRD) were used to determine the physio-chemical properties of the Pt/Al_2O_3 catalyst. Multipoint Brunauer-Emmett-Teller (BET) provided information regarding the surface are and pore size of the catalyst. XRD patterns were recorded at room temperature, using a Panalytical MPD diffractometer equipped with an X′ Celerator detector and secondary monochromator in Bragg–Brentano geometry. $CuK\alpha_{1,2}$ radiation, λ_1= 1.5406 Å, λ_2= 1.5444 Å, a step size of 0.017◦ and 100 s/step were used. Rietveld refinements were performed using PowderCell 2.4 to calculate Pt crystallite size. A ChemBET Pulsar TPR/TPD instrument equipped with a thermal conductivity detector (TCD) was used to perform H2-TPR experiments. Approximately 25 mg of catalyst was placed in a U-shaped quartz tube reactor and held in place with quartz wool. The sample was heated from 50 °C to 450 °C at a heating rate of 5 °C·min^{-1} under the constant H_2/Ar (1:9) flow. Multipoint BET surface are measurements were performed on a Quantachrome Autosorb AS-1 instrument at -196 ºC. Prior to the analysis the samples were outgassed in vacuum at 200 ºC for 4 h. The H2 - TPR of a 5 wt. % Pt/Al_2O_3 sample is displayed in Figure 2; it exhibits the presence of a single sharp peak at *ca*. 300 °C and starting at 250 °C and ending at 325 °C. The presence of this single sharp peak indicates that only one type of active metal is present in the catalyst. The result of TPR is in good agreement with the XRD of the catalyst, showing only Pt and alumina in the catalyst – discussed below.

The information regarding the reducibility of Pt/Al_2O_3 was used to activate the catalyst *in-situ* before the APR tests. Controlling the reduction temperature is important since the catalyst reduction (activation process) is an exothermic process that influences the catalyst's ability to perform the reforming reaction. Since small catalyst particle sizes are more prone to sintering, the reduction process was performed using diluted hydrogen at 300 °C.

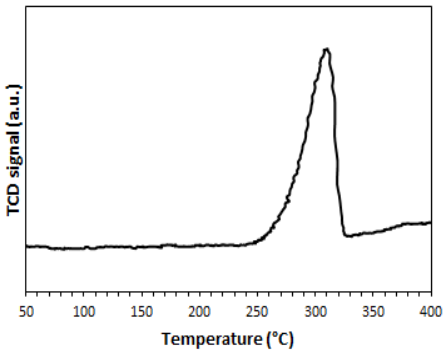

Figure 2. H2 - TPR of a 5 wt. % Pt/Al_2O_3 catalyst sample.

XRD patterns of fresh and spent Pt/Al_2O_3 samples are shown in figure 3. The spent catalyst was subjected to methanol APR for 7.5 hours at 230 ºC and 3.2 MPa using a 5 wt. % methanol

aqueous solution supplied at 0.3 (h^{-1}) WHSV. Comparing fresh and spent catalysts, the XRD diffractogram of the spent sample shows that alumina support underwent phase change and Pt metal was sintered and leached.

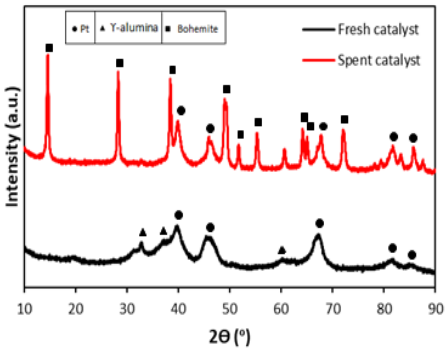

Figure 3. XRD diffractograms of fresh (black line) and spent (red line) Pt/Al_2O_3 samples.

In both fresh and spent catalysts, characteristic Pt metallic peaks were detected at 2θ = 39.8 º, 46.5 º, and 67.8 º (JCPDS 01-1190) [1]. However, these peaks are broader for the fresh catalyst compared to the spent catalyst. These could be due to poor crystallinity, overlapping with alumina peaks, or undetectable Pt size due to well-dispersed particles in the fresh catalyst. The calculated Pt particle size using the William-Hall method was estimated to be *ca*. 5 nm in the fresh catalyst sample, as shown in Table 1.

The spent catalyst has a Pt crystal size of *ca*. 12 nm, indicating that Pt particles were sintered under the APR reaction conditions. The calculated amount of Pt in the fresh catalyst was 4.5 wt. %, which is according to the value reported by the catalyst supplier. However, the spent catalyst showed approximately 3 wt. % of Pt mass in the catalyst. Suggesting that leaching of Pt occurred during the APR reaction. Moreover, the spent catalysts showed peaks related to boehmite, while fresh catalyst only shows peaks for γ-alumina. The presence of this crystalline structure shows that alumina was transformed in boehmite, which is a thermodynamically more stable phase under high humidity levels, such as under APR reaction conditions.

Table 1. Pt crystallize size and mass fraction of a fresh and spent catalyst derived from XRD analysis.

Pt Crystallite size (nm)	**Fresh catalyst**	**Spent catalyst**
	5 (± 2)	12 (±1)
Pt mass fraction (%)	**Fresh catalyst**	**Spent catalyst**
	4.5 (± 0.5)	3.1 (±1)

The N2 adsorption-desorption isotherm for the catalyst Pt/Al_2O_3 is shown in figure 4 and the BET surface area, average pore size and pore volume are listed in table 2.

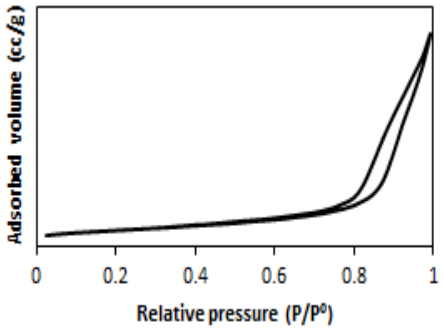

Figure 4. Nitrogen adsorption-desorption isotherm and pore size distribution of Pt/Al_2O_3.

Table 2. Physicochemical properties of Pt/Al_2O_3.

Pt/Al_2O_3	BET surface area (m^2/g)	Pore volume (cc/g)	Pore diameter (nm)
	205.9	0.8	13.0

According to IUPAC classification, Pt/Al_2O_3 has a type (IV) isotherm which indicates the mesoporous structure of the catalyst with the pore size wider than 4 nm. The catalyst also showed an H3 type hysteresis loop. This is usually observed for the irregular pore system with agglomerated particles that are slit-shaped pores of irregular sizes or shapes [2].

3.2. Pt/Al_2O_3 activity and effect of the operating temperature

The effect of temperature on methanol APR conversion is depicted in Figure 5 for temperatures 190 °C, 210 °C, and 230 °C. Both reforming and WGS reactions are kinetically favored at higher temperatures. Unfortunately, undesirable side reactions, such as methanation, are also thermodynamically favored by high temperatures. An increase in the experimental methanol conversion was observed at higher temperatures. At low temperatures (190 °C), the methanol conversion does not go above 15 %, even at very low WHSV. Compared with the MSR, the performance of methanol APR is lower; for a WHSV of 1 h^{-1} and at 190 °C, the methanol conversion is *ca*. 75 % for MSR [3], while for APR is less than 5 %. For the 55 wt. % feed methanol aqueous solution, the resulting APR conversion was even lower. WHSV is defined as the weight of feed (methanol) flowing per unit weight of the catalyst per hour. As expected, at the same WHSV with varied methanol concentration and feed flow rate, the methanol conversion is similar. It is noticeable that for the same WHSV, the feed flow rate is very

different for 5 wt. % and 55 wt. % aqueous methanol solution. However, the methanol conversion does not vary for the same WHSV, making the methanol dilution effect on conversion negligible.

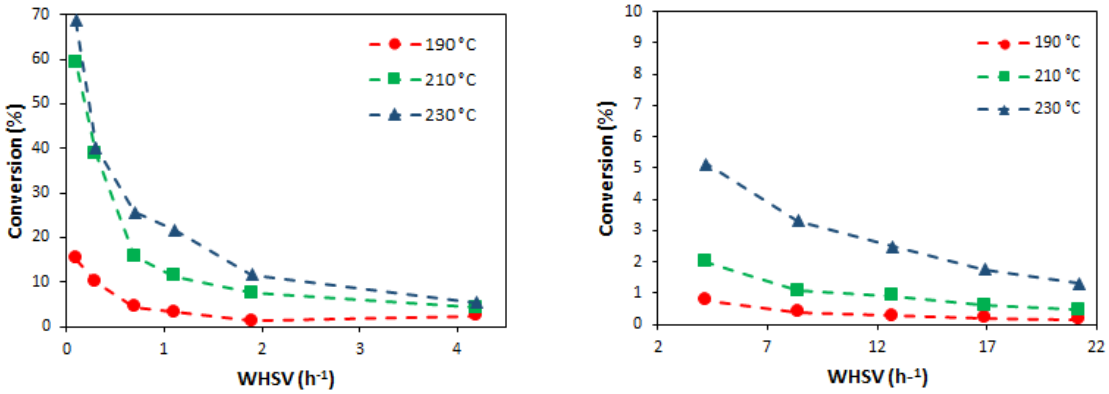

Figure 5. Methanol conversion in aqueous-phase reforming of (a) 5 wt. % and (b) 55 wt. % aqueous methanol aqueous solution over 5 wt. % Pt/Al_2O_3, N2 co-feeding of 30 ml·min^{-1}; and operating temperatures of 190 °C, 210 °C, and 230 °C as a function of WHSV. Operating pressure of (a) 3.2 MPa and (b) 6.0 MPa.

APR has the potential to be integrated with an HT-PEMFC system due to its higher energy efficiency and simple recycling of unreacted reagents; this allows the APR to operate at conversions lower than 100 % without significantly affecting the system efficiency. Moreover, HT-PEMFCs have a high tolerance to reforming contaminants (up to 3 % [4], [5]).

For 55 wt. % methanol feed aqueous solution the maximum hydrogen production rate was *ca.* 500 mol·min^{-1}·g$^{-1}_{cat}$. As depicted in Figure 6, the hydrogen production rate as a function of the WHSV peaks at WHSV ≈ 13 h^{-1}, especially for 210 °C and 230 °C, decreasing slightly afterward. At higher methanol concentrations and for the same feed flow rate, the contact time between reactants and catalyst decreases, which adversely affects hydrogen production [6]. In comparison, for the same operating conditions, MSR has an hydrogen production rate of 2-3 times higher [7].

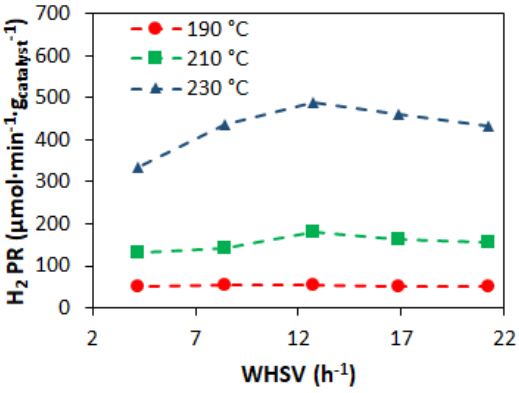

Figure 6. Hydrogen production rate in aqueous-phase reforming of 55 wt. % methanol feed aqueous solution over 5 wt. % Pt/Al_2O_3, N2 co-feeding of 30 ml·min^{-1}; and operating temperatures of 190 °C, 210 °C, and 230 °C at various residence times. Operating pressure 6.0 MPa.

3.3. Effect of the operating pressure

It is important to study the reaction pressure on APR performance since APR is a multiphase system with a reaction often controlled by a mass transport-limited regime. Figure 7 shows the effects of operating pressure on methanol conversion at 230 °C. For a methanol feed concentration of 5 wt. %, the methanol conversion decreased from 25 % at 3.2 MPa to 13 % at 4.0 MPa, while for a methanol feed concentration of 55 wt. %, the methanol conversion is mostly constant with the reaction pressure. In multiphase systems, pressure affects density, bubble size distribution [8], [9], and catalyst-wetting efficiency [10]. While the wetting efficiency increases with pressure [10], which is crucial for multiphase systems, increasing the operating pressure, increases the hydrogen partial pressure which affects negatively the reaction rate [11]. Hydrogen has very low solubility in water and methanol, and diffuses slowly from the catalyst active site, where it is formed, to the bulk [12]; moreover, high pressure reduces the bubble size reducing the bubble disengaging rate. In this sense, the catalyst surface active sites are occupied for a longer time. In addition, the hydrogen availability near an active site can promote the hydrogenation of intermediate species, leading to a loss in selectivity. Since nitrogen (carrier gas) is also not soluble in the liquid reaction phase, it should leave the reactor mixed with hydrogen and CO_2, besides water and methanol vapor. Performing the methanol-reforming reaction below the bubble point pressure (gaseous methanol reforming) did not yield conversions higher than the observed for methanol APR. The methanol conversion achieved by APR and by MSR was *ca*. 2 % with no significant influence of the pressure (Figure 7b).

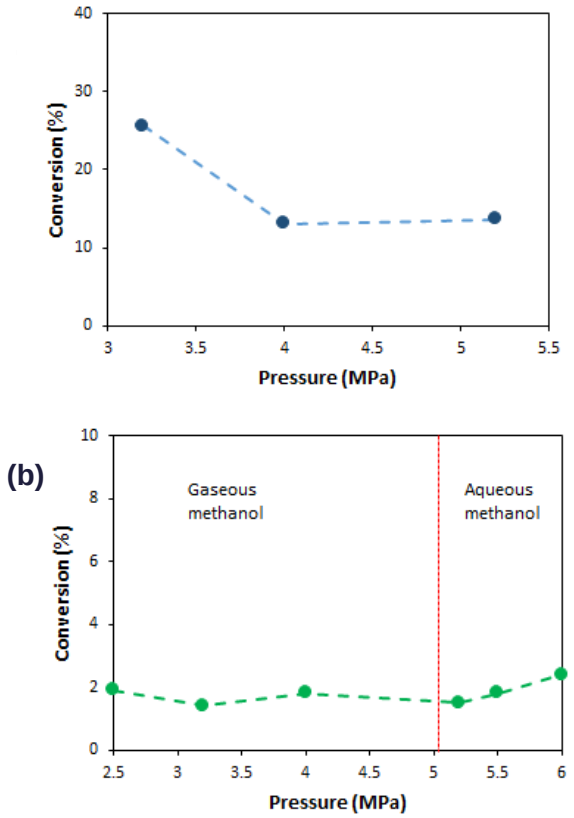

Figure 7. Methanol conversion as a function of pressure for (a) 5 wt. % and (b) 55 wt.% methanol aqueous solution over 5 wt. % Pt/Al_2O_3 catalyst. Operating temperature of 230 °C, residence time of (a) 0.7 h^{-1} and (b) 12.7 h^{-1}.

3.4. Pt/Al_2O_3 catalyst selectivity for methanol APR

A high methanol APR selectivity to hydrogen originates an energy conversion efficiency – from methanol to hydrogen – and allows feeding directly the reformate to an HT-PEMFC system. Apart from the nature of the catalyst – both metal and support, the selectivity of hydrogen depends on the operating conditions [13]. Figure 8 shows the selectivity of hydrogen as a function of residence time under various operating pressures.

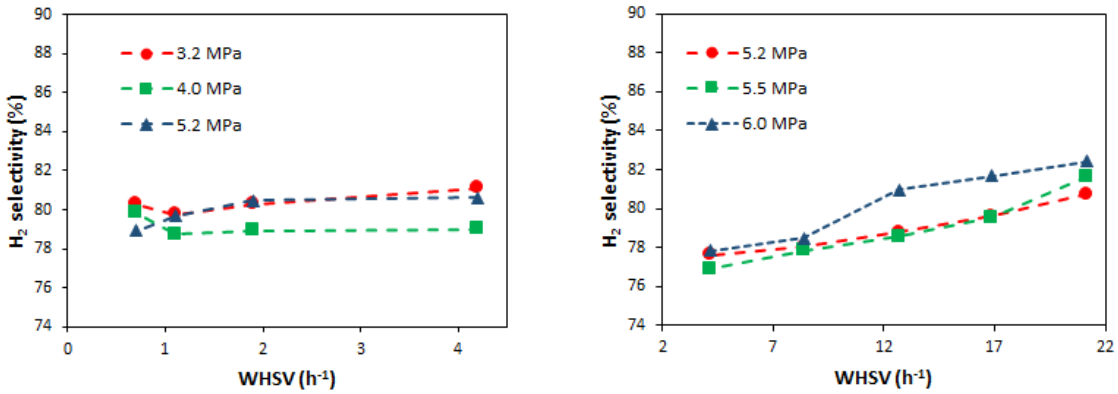

Figure 8. H2 selectivity in aqueous-phase reforming of (a) 5 wt. % and (b) 55 wt. % methanol aqueous solution on a 5 wt. % Pt/Al_2O_3 catalyst, with a N2 co-feeding of 30 ml·min^{-1} and at 230 °C, for at various pressures and as a function of WHSV.

For 5 wt. % and 55 wt. % methanol feed aqueous solution, the selectivity to hydrogen ranged between 77 % - 82 %. Operating pressure had a small effect on the selectivity of hydrogen while it depends more on the WHSV. For low WHSV values, the selectivity to hydrogen is mostly independent of the methanol conversion. Therefore, it can be concluded that hydrogen production over Pt/Al_2O_3 is not restricted by the hydrogenation of CO/CO_2. The selectivity to hydrogen is above 75 % for all experiments, indicating that $H2/CO_2$ ratio for these experiments stayed above a factor of 3.

Apart from the nature of the catalyst (both metal and support) and operating conditions, the reactor design has also been studied to increase the selectivity of hydrogen. It is reported that using a microchannel reactor instead of an FBR, the selectivity to hydrogen becomes higher by a factor of two, regardless of the feedstock conversion. The selectivity to hydrogen in a microchannel reactor should increase because of a better catalyst wettability, making the mass transport of the products easier, namely the transport of hydrogen [14].

3.5. Pt/Al_2O_3 catalyst stability

The long-term stability of methanol APR was performed to study the effects on catalyst performance and methanol conversion. Figure 9 shows the methanol conversion as a function of time for a 5 wt. % methanol feed aqueous solution. Steady-state performance was achieved for >7 h.

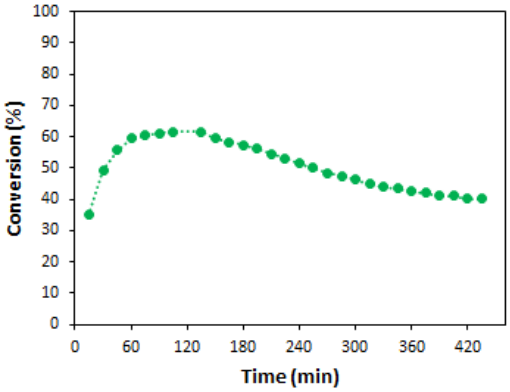

Figure 9. Methanol conversion as a function of time for 5 wt. % methanol aqueous solution over 5 wt. % Pt/Al_2O_3 at 230 °C and 3.3 MPa and 0.3 (h^{-1}) WHSV.

The catalytic activity increased at the beginning and then slowly decreased until a steady state. The catalytic activity (methanol conversion) decrease was assigned to the transformation of alumina support to boehmite, metal phase sintering, and Pt leaching, as discussed earlier. Due to the shortcomings and poor performance of Pt/Al_2O_3 catalyst, further studies carried out to optimize a Pt-based catalyst that shows higher APR activity.

4. Metal aluminate supported on Pt-based catalysts

APR operating conditions hinders the performance of Pt/Al_2O_3. Pt/Al_2O_3 suffers from sintering and leaching of Pt, and alumina phase changes to boehmite (γ-AlOOH) under hydrothermal conditions of APR. Additionally, acidic supports such as Al_2O_3 tends to favor higher alkane formation compared to neutral or basic supports [15]. To improve the catalyst activity and stability, various supports have been used instead of metal oxides. Molybdenum carbide (MoC) [16] and nickel aluminate ($NiAl_2O_4$) [17] supported Pt-based catalyst are the highest performing catalysts reported for methanol APR. Li *et al*. [17] reported four times higher H_2 yield with $Pt/NiAl_2O_4$ compared to Pt/Al_2O_3. Therefore, different metal-aluminate based supports were synthesized to prepare Pt-based catalysts and the performance for APR was evaluated.

All reagents were used in their pristine condition. Metal aluminate supports were synthesized using the co-precipitation method. A certain amount of metal nitrate (Metal = Ni, La, Cu, Mg, Co) and aluminum nitrate were dissolved in deionized water at room temperature. After, aqueous ammonia solution (32 wt. % NH_3) was added to this solution drop by drop until pH reached

8. Formed precipitates were continuously stirred and aged overnight at room temperature. Later, the precipitates were filtered, washed (until pH 7), and dried (100 °C for 12 h) in flowing air. Finally, the support was calcined at 800 °C (3 °C·min^{-1}) for 8 h in a flowing N2 (120 mL·min^{-1}) atmosphere. For all the synthesized supports, Metal/Al stoichiometric ratio was kept at 1:2. Prepared metal aluminate support and Pt precursor were used to synthesize catalysts via the incipient wetness impregnation (IWI) method. A certain amount (for 2 wt. % Pt loading) of tetraammineplatinum (II) nitrate was added to deionized water and mixed. A certain amount of metal aluminate support was added to this aqueous solution and stirred. The slurry was dried (100 °C for 12 h) and calcined (450 °C for 5 h) in static air to obtain the catalyst. The catalyst was reduced *in-situ* prior to the methanol APR tests.

4.1. Textural properties of metal-aluminate support

Multipoint BET surface are measurements were performed on a Quantachrome Autosorb AS-1 instrument at -196 °C. Prior to the analysis the samples were outgassed in vacuum at 200 °C for 4 h. The N_2 adsorption-desorption isotherm for these supports are shown in figure 10 and the BET surface area, average pore size and pore volume are listed in table 3.

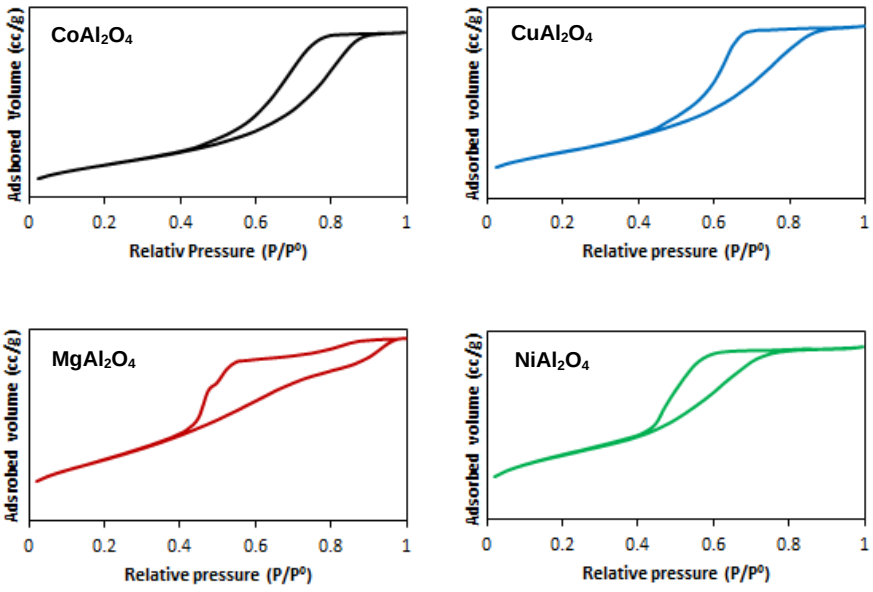

Figure 10. Nitrogen adsorption-desorption isotherm of $CoAl_2O_4$, $CuAl_2O_4$, $MgAl_2O_4$ and $NiAl_2O_4$.

According to IUPAC classification, all the synthesized supports have a type IV isotherm which indicates the mesoporous structure of the catalyst with pore size wider than 4 nm. $CoAl_2O_4$, $CuAl_2O_4$ and $NiAl_2O_4$ showed a more distinctive type IV(a) isotherm. This type of isotherm is attributed to a relatively weak adsorbent-adsorbate interaction. At higher relative pressure, molecular clustering is followed by pore filling. In general, type IV isotherm is also observed

on hydrophobic mesoporous material. $MgAl_2O_4$ also showed type IV(a) isotherm, however, less defined at high relative pressure. $CoAl_2O_4$, $CuAl_2O_4$ and $NiAl_2O_4$ presented type H1 hysteresis loop which is associated with materials exhibiting a narrow range of uniform mesopores. Similarly, H1 loop is also found in networks of ink-bottle pores where the width of the neck size distribution is similar to width of the pore/cavity size distribution. Whereas, $MgAl_2O_4$ showed a type H3 hysteresis loop, indicating a non-rigid aggregates of plate-like particles. For type H3 loop materials, the pore network consists of macropores which are not completely filled with pore condensate. Table 3 shows the BET surface are, pore volume and pore diameter for the synthesized supports. $CuAl_2O_4$ showed the highest surface are and pore volume. Whereas, $CoAl_2O_4$ had the lowest surface are with highest pore diameter noted.

Table 3. Physicochemical properties of $CoAl_2O_4$, $CuAl_2O_4$, $MgAl_2O_4$ and $NiAl_2O_4$.

	BET surface area (m^2/g)	**Pore volume (cc/g)**	**Pore diameter (nm)**
$CoAl_2O_4$	146.9	0.2	6.2
$CuAl_2O_4$	370.4	0.4	5.7
$MgAl_2O_4$	217.9	0.2	3.7
$NiAl_2O_4$	160.8	0.1	3.7

4.2. Catalytic Activity test

The catalytic activity tests for the synthesized catalysts were measured at 230 ^oC and at 6.0 MPa for 55 wt. % methanol aqueous solution. Only 55 wt. % methanol aqueous solution was used to mimic the real conditions of the EMPOWER CHP reformer system. Various residence times (2.5 – 12.7 h^{-1} WHSV) were used to characterize catalyst performance. The catalytic activity tests were evaluated in terms of methanol conversion and hydrogen production rate.

An increase in methanol conversion was observed with the increasing residence times as expected. Figure 11 shows the methanol conversion as a function of residence times for various metal aluminate supported Pt-based catalysts.

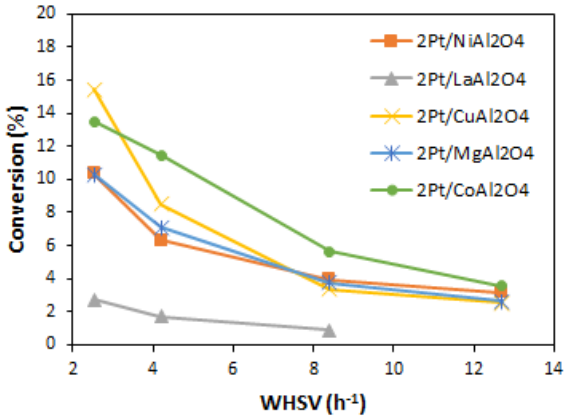

Figure 10. Methanol conversion in aqueous-phase reforming of a 55 wt. % aqueous methanol aqueous solution, N_2 co-feeding of 30 ml·min^{-1}; and operating temperatures 230 °C as a function of WHSV. Operating pressure 6.0 MPa

Pt supported on $CuAl_2O_4$ and $CoAl_2O_4$ showed the highest methanol conversation while $Pt/LaAl_2O_4$ showed the lowest methanol conversation (under 5 %) even at increased residence times. At lower residence times, all the catalyst showed almost the same methanol conversion. Pt supported on $NiAl_2O_4$ and $MgAl_2O_4$ showed a very similar catalytic activity across all the residence times. Interesting, both supports also displayed the same pore size and pore volume. Pt/NiAl2O4 is the highest performing methanol APR catalyst reported in literature [17]. It is noticeable that the synthesized catalyst has outperformed the $Pt/NiAl_2O_4$ catalyst. Additionally, all the catalysts significantly outperformed the commercial Pt/Al_2O_3 as well. At the same operating conditions, the in-lab catalysts showed 2 times higher activity than the commercial catalyst. It is also interesting to notice that the synthesized catalyst has 2 wt. % Pt loading while the commercial catalyst contains 5 wt. % Pt loading.

Figure 11 shows the catalytic evaluation results in hydrogen production rate as a function of WHSV (230 ^{o}C, 6.0 MPa).

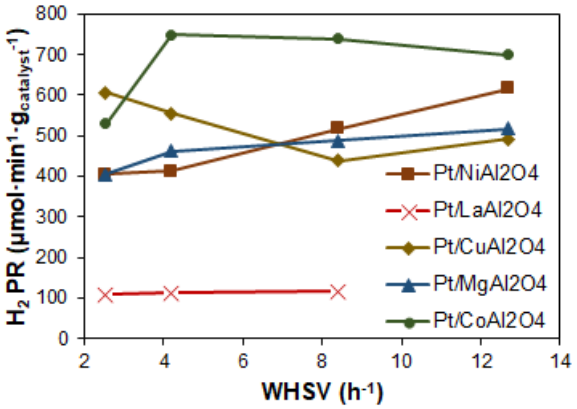

Figure 11. Hydrogen production rate in aqueous-phase reforming of a 55 wt. % aqueous methanol aqueous solution, N2 co-feeding of 30 ml·min^{-1}; and operating temperatures 230 °C as a function of WHSV. Operating pressure 6.0 MPa

The prepared catalysts showed high activities with the highest hydrogen PR being *ca.* 750 µmol·min^{-1}·$g_{catalyst}^{-1}$ achieved over Pt/$CoAl_2O_4$. The hydrogen production rate mostly remained constant even with the decreased residence ties with for most of the catalyst. However, the hydrogen production rate over Pt/$NiAl_2O_4$ showed slight increase at higher WHSV. On the other hand, Pt/$LaAl_2O_4$ showed the lowest hydrogen PR over the various residence times. The high hydrogen production rate achieved by these catalysts indicates that high activity in reforming reactions was followed by high activity in water-gas shift reaction. The high performance of these catalysts can be attributed to the high thermal stability, low surface acidity, and spinel structure of the metal aluminate support. Additionally, a large number of oxygen vacancies and high synergy between Pt and metal aluminate support reduces PtOx to Pt. Thus, making Pt more stable and active for APR performance.

5. Conclusions

The catalytic activity of Pt/Al_2O_3 catalyst on the methanol aqueous phase reforming reaction was lower than initially expected. The experiments reported in literature, uses very low concentrated methanol solutions which can lead to wrong interpretations in terms of catalyst activity. Nevertheless, significant efforts were made by the research team, to find an alternative solution that math the projects requirements. Pt/MoC (reported D2.2), show higher activity than other catalyst reported in the literature, but it presents several disadvantages. First it has a very high reduction temperature (700 °C) and it oxidizes with air at room environment conditions. Second, the production process is very time consuming, with several steps. Third, is

energy intensive with long processes at high temperatures. Fourth, this catalyst used expensive precursors such as $H_2PtCl_6 \cdot 6H_2O$.

Besides, molybdenum carbide (MoC), different metal-aluminate (Metal = Ni, La, Cu, Mg, Co) based supports were synthesized by co-precipitation method to prepare Pt-based catalysts. The $Pt/CuAl_2O_4$ and $Pt/CoAl_2O_4$ showed the highest methanol conversation and clearly outperform the commercial (Pt/Al_2O_3). Despite the good results, the catalyst activity still requires further improvements, so this process (APR) can represent a feasible and more efficient alternative to gas-phase reforming.

6. References

[1] M. El Doukkali *et al.*, “Deactivation study of the Pt and/or Ni-based γ-Al2O 3 catalysts used in the aqueous phase reforming of glycerol for H2 production,” *Applied Catalysis A: General*, vol. 472. pp. 80–91, 2014. doi: 10.1016/j.apcata.2013.12.015.

[2] M. Thommes *et al.*, “Physisorption of gases , with special reference to the evaluation of surface area and pore size distribution (IUPAC Technical Report),” vol. 87, pp. 1051–1069, 2015, doi: 10.1515/pac-2014-1117.

[3] P. Ribeirinha, C. Mateos-Pedrero, M. Boaventura, J. Sousa, and A. Mendes, “CuO/ZnO/Ga2O3 catalyst for low temperature MSR reaction: Synthesis, characterization and kinetic model,” *Appl. Catal. B Environ.*, vol. 221, no. September 2017, pp. 371–379, 2018, doi: 10.1016/j.apcatb.2017.09.040.

[4] P. Ribeirinha, M. Abdollahzadeh, A. Pereira, F. Relvas, M. Boaventura, and A. Mendes, “High temperature PEM fuel cell integrated with a cellular membrane methanol steam reformer: Experimental and modelling,” *Appl. Energy*, vol. 215, no. September 2017, pp. 659–669, 2018, doi: 10.1016/j.apenergy.2018.02.029.

[5] Q. Li, R. He, J.-A. Gao, J. O. Jensen, and N. J. Bjerrum, “The CO Poisoning Effect in PEMFCs Operational at Temperatures up to 200°C,” *J. Electrochem. Soc.*, vol. 150, no. 12, p. A1599, 2003, doi: 10.1149/1.1619984.

[6] J. W. Shabaker, R. R. Davda, G. W. Huber, R. D. Cortright, and J. A. Dumesic, “Aqueous-phase reforming of methanol and ethylene glycol over alumina-supported platinum catalysts,” *J. Catal.*, 2003, doi: 10.1016/S0021-9517(03)00032-0.

[7] P. Ribeirinha, C. Mateos-Pedrero, M. Boaventura, J. Sousa, and A. Mendes, “CuO/ZnO/Ga2O3 catalyst for low temperature MSR reaction: Synthesis, characterization and kinetic model,” *Appl. Catal. B Environ.*, vol. 221, no. July 2017, pp. 371–379, 2018, doi: 10.1016/j.apcatb.2017.09.040.

[8] I. Iliuta, “Performance of fixed bed reactors with two-phase upflow and downflow,” *J. Chem. Technol. Biotechnol.*, vol. 68, no. 1, pp. 47–56, 1997, doi: 10.1002/(SICI)1097-4660(199701)68:1<47::AID-JCTB603>3.0.CO;2-P.

[9] I. Iliuta and F. C. Thyrion, “Flow regimes, liquid holdups and two-phase pressure drop for two-phase cocurrent downflow and upflow through packed beds: Air/Newtonian and non-Newtonian liquid systems,” *Chem. Eng. Sci.*, vol. 52, no. 21–22, pp. 4045–4053, 1997, doi: 10.1016/S0009-2509(97)00247-9.

[10] M. P. Dudukovic, F. Larachi, and P. L. Mills, “Multiphase reactors - revisited,” *Chem. Eng. Sci.*, vol. 54, no. 13–14, pp. 1975–1995, 1999, doi: 10.1016/S0009-2509(98)00367-4.

[11] J. W. Shabaker, G. W. Huber, and J. A. Dumesic, “Aqueous-phase reforming of oxygenated hydrocarbons over Sn-modified Ni catalysts,” *J. Catal.*, vol. 222, no. 1, pp. 180–191, 2004, doi: 10.1016/j.jcat.2003.10.022.

[12] J. W. Shabaker and J. A. Dumesic, “Kinetics of aqueous-phase reforming of oxygenated hydrocarbons: Pt/Al 2O3 and Sn-modified Ni catalysts,” *Ind. Eng. Chem. Res.*, vol. 43, no. 12, pp. 3105–3112, 2004, doi: 10.1021/ie049852o.

[13] R. R. Davda, J. W. Shabaker, G. W. Huber, R. D. Cortright, and J. A. Dumesic, “A review of catalytic issues and process conditions for renewable hydrogen and alkanes by aqueous-phase reforming of oxygenated hydrocarbons over supported metal catalysts,” *Appl. Catal. B Environ.*, vol. 56, no. 1-2 SPEC. ISS., pp. 171–186, 2005, doi: 10.1016/j.apcatb.2004.04.027.

[14] M. F. Neira D’Angelo, V. Ordomsky, J. Van Der Schaaf, J. C. Schouten, and T. A. Nijhuis, “Aqueous phase reforming in a microchannel reactor: The effect of mass transfer on hydrogen selectivity,” *Catal. Sci. Technol.*, vol. 3, no. 10, pp. 2834–2842, 2013, doi: 10.1039/c3cy00577a.

[15] P. Lakhtaria, P. Ribeirinha, W. Huhtinen, S. Viik, J. Sousa, and A. Mendes, “Hydrogen production via aqueous-phase reforming for high-temperature proton exchange membrane fuel cells - a review,” *Open Res. Eur.*, vol. 1, p. 81, 2022, doi: 10.12688/openreseurope.13812.3.

[16] L. Lin *et al.*, “Low-Temperature hydrogen production from water and methanol using Pt/α-MoC catalysts,” *Nature*, vol. 544, no. 7648, pp. 80–83, 2017, doi: 10.1038/nature21672.

[17] D. Li *et al.*, “NiAl2O4 Spinel Supported Pt Catalyst: High Performance and Origin in Aqueous-Phase Reforming of Methanol,” *ACS Catal.*, vol. 9, no. 10, pp. 9671–9682, 2019, doi: 10.1021/acscatal.9b02243.